Probing the Surface Chemical Structure of the Novel Biodegradable Polymer Poly(β-malic acid) and Its Ester Derivatives Using ToF-SIMS and XPS

S. R. Leadley,[†,‡] M. C. Davies,[*,‡] M. Vert,[§] C. Braud,[§] A. J. Paul,[∥] A. G. Shard,[‡] and J. F. Watts[⊥]

Laboratory of Biophysics and Surface Analysis, Department of Pharmaceutical Sciences, University of Nottingham, Nottingham NG7 2RD, U.K., CRBA.CNRS Faculty of Pharmacy, The University of Montpelier, 1, 15 Avenue Charles Flahault, 34060 Montpelier, France, C.S.M.A. Ltd., Armstrong House, Oxford Road, Manchester M1 7ED, U.K., and Department of Materials Science and Engineering, University of Surrey, Guildford, Surrey GU2 5XH, U.K.

Received February 25, 1997; Revised Manuscript Received August 19, 1997[⊗]

ABSTRACT: Poly(β-malic acid) and its ester derivatives are biodegradable polyesters, which are candidates for innovative drug delivery systems. XPS and ToF-SIMS have been used to investigate the surface chemical structure of poly(β-malic acid), its butyl and benzyl ester derivatives, and a range of their copolymers. The XPS analysis of these polymers showed a good correlation between the experimental and theoretical compositions. The peak-fitting routine applied to the C 1s spectra provided functional group information. The ToF-SIMS analysis of these materials showed characteristic fragmentation patterns for each homo- and copolymer, which consisted of ions diagnostic of the polymers under investigation. This combined use of ToF-SIMS and XPS is shown to provide a detailed insight into the surface chemical structure of the poly(β-malic acid) polymers.

Introduction

The use of biodegradable polymers for the development of temporary surgical and pharmaceutical devices like sutures, absorbable bone plates, and devices for controlled release of drugs is continually growing.[1] For each biomedical application, the material properties of the polymer will differ. This has resulted in the synthesis of a wide range of biodegradable polymers with a variety of properties. By definition, biodegradable polymers are "polymeric systems or devices which can be attacked by biological elements so that the integrity of the system is affected and gives fragments or other degradation by-products".[1] However, the fragments may be removed from the site of action but not necessarily from the body. Any biomedical material should meet the criterion that any degradation product should not be toxic; thus, biodegradable polymers used in biomedical applications should ideally be "bioresorbable". That is, the degradation products should be low molecular weight compounds which may be eliminated from the body through natural pathways.[1,2] Although many chemical linkages are cleavable under physiological conditions, they are limited to esters, ortho esters, anhydrides, and phosphazenes if the polymer is to be bioresorbable. This has led to a model for an ideal biodegradable polymer as shown schematically below.[1]

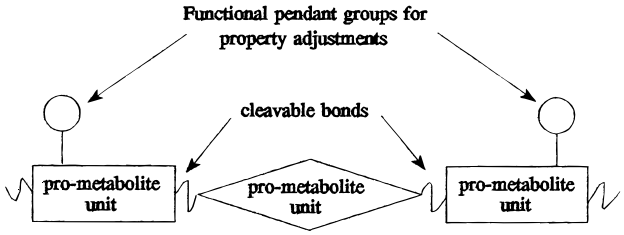

The above model requires that biodegradable polymers should consist of backbone building blocks that may be eliminated naturally via cleavable bonds. The building blocks should ideally possess some form of functional group that may be manipulated so as to allow property adjustment for the polymers.

A class of biodegradable polymer that has attracted considerable attention for the design of novel drug delivery systems is the polyesters. These include poly(α-hydroxy acids),[3] poly(β-hydroxy acids),[4] poly(α-malic acids),[5] pseudopoly(α-amino acids),[6] and their copolymers.[7] Of particular interest are the polyesters with pendant carboxylic acid groups. These carboxylic acid groups may be functionalized to manipulate material properties and are thought to have a catalytic effect on the hydrolytic scission of the ester bonds, increasing the degradation rate.[3]

The polyesters of interest here are the poly(β-hydroxy acids) derived from malic acid of the general structure below.

* To whom correspondence should be addressed.
[†] Current address: Dow Corning Limited, Barry, South Glamorgan CF63 2YL, U.K.
[‡] University of Nottingham.
[§] The University of Montpelier.
[∥] C.S.M.A. Ltd.
[⊥] University of Surrey.
[⊗] Abstract published in *Advance ACS Abstracts,* October 1, 1997.

S0024-9297(97)00261-1 CCC: $14.00

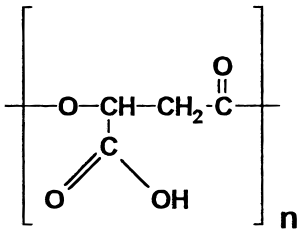

The synthesis of linear polyesters from malic acid is not possible via step growth polymerization, due to its trifunctionality, which leads to cross-linked systems. Also, the ring-opening polymerization of malolactonic acid is not possible as the pendant acid group interacts with the initiator, precluding polymerization.[2] However, in 1978, the synthesis of linear polyesters derived from malic acid was achieved by using ring-opening polymerization of racemic β-benzyl malolactonate, a carboxyl-protected derivative of malolactonic acid. This synthetic route started from racemic bromosuccinic acid yielding poly(benzyl β-malate) in a four-step process, as shown in Scheme 1.[4] Another synthetic route has also been developed, starting from aspartic acid, as shown in Scheme 2.[8] Both synthetic routes yield poly(benzyl β-malate), which is converted to poly(β-malic acid) through the catalytic hydrogenolysis of the side chain protecting group. The use of a heterogeneous palladium/carbon catalyst for hydrogenolysis appeared to be main chain ester bond respecting and allowed selective and total cleavage of the protecting groups. Thus, the simple synthesis of (benzyl ester β-malate)-*co*-(β-malic acid) copolymers ($PMLABz_{1-x}H_x$) is possible. This results in the relatively easy manipulation of the material properties of these linear polyesters. Due to poly(β-malic acid) and its derivatives being bioresorbable and hydrolytically sensitive, they have been chosen as candidates for novel drug delivery systems.[9]

The importance of the surface composition of solid materials has been recognized for some time. The composition of the topmost atomic layers of solid materials is crucial in the understanding of technologically important processes such as oxidation, corrosion, catalysis, adhesion, thermionic emission, crystal growth, etc.[10] It has been proposed that the surface of a solid be considered as a fourth state of matter, a zone with unique chemistry, organization, dynamics, and electrical properties.[11] Therefore, when characterizing any new material, its surface properties should be determined as well as its bulk properties. The difference between the surface and bulk structures of synthetic materials can be related to a number of factors, including the following: the accessibility of molecules at the surface interface leading to surface reaction and surface energy minimization by mobility, additive migration, and environmental contamination.[12]

A single surface analysis method will rarely provide sufficient information to understand the surface chemical structure of a material completely. Therefore, a multitechnique approach should be used, as it will yield pieces of information that can be integrated to provide a more complete picture of the surface.[13] As both secondary ion mass spectrometry (SIMS) and X-ray photoelectron spectroscopy (XPS) have been successfully used for the characterization of other polyesters,[14,15] it is anticipated that these techniques will provide information as to the surface composition of the homopolymers poly(β-malic acid), poly(benzyl β-malate), poly(butyl β-malate), and their copolymers, as listed in Table 1.

Scheme 1. Synthetic Route for Poly(β-malic acid) from Bromosuccinic Acid[4]

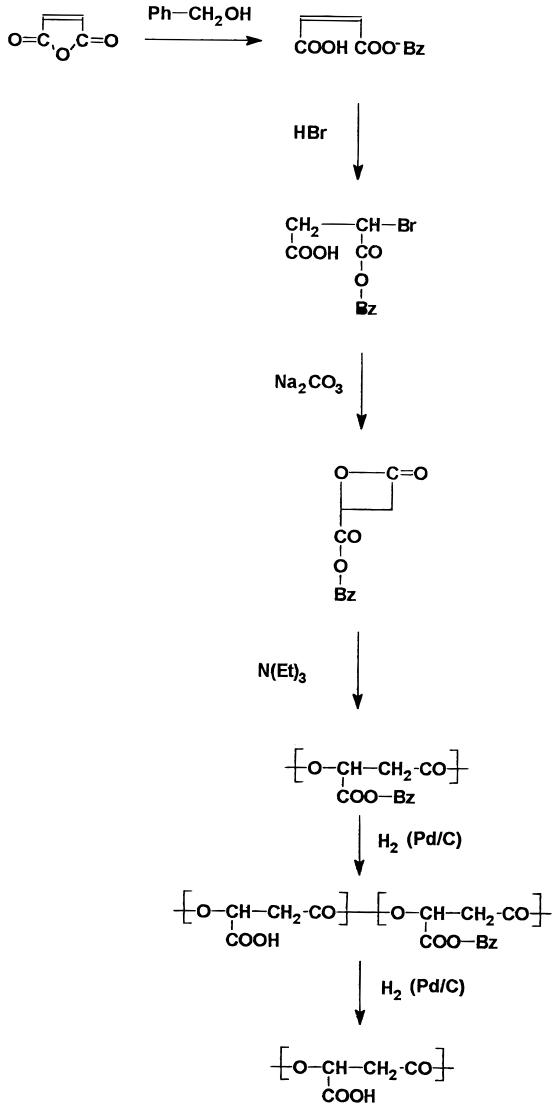

Materials and Methods

Polymer Synthesis and Sample Preparation. The poly(β-hydroxy acids) were prepared by the method first described by Guerin et al.,[8] using the synthetic route starting with aspartic acid as shown in Scheme 2. This synthetic route produces l-(−)-bromosuccinic acid from aspartic acid and NaBr in sulfuric acid and $NaNO_2$, which is converted to l-(+)-bromosuccinic anhydride in anhydrous tetrahydrofuran (THF) and trifluoroacetic acid. Benzyl malolactonate and butyl malolactonate are then prepared by reacting the bromosuccinic anhydride with benzyl alcohol and butyl alcohol, respectively. Poly(benzyl β-malate) and poly(butyl β-malate) homopolymers and their copolymers are produced by polymerizing their respective malolactonates at 70 °C under nitrogen using triethylamine as an initiator. The conversion of poly(benzyl β-malate) to poly(β-malic acid) and its copolymers was carried out by catalytic hydrogenolysis in *N*-methylpyrolidone at room temperature using a 10% palladium−charcoal catalyst.

Spectroscopy. The XPS spectra were acquired using a VG Scientific ESCALAB Mk II electron spectrometer, employing Mg kα X-rays ($h\nu = 1253.6$ eV). The X-ray gun was operated at 120 W and placed relative to the sample to give a 45° electron take-off angle, thus analyzing the environments of elements present in the top 50 Å of the polymer surface. Survey spectra (0−1000 eV) and narrow scans in the C 1s and

Table 1. Poly(β-hydroxy acids) under Investigation

polymer	copolymer ratio: benzyl β-malate	copolymer ratio: butyl β-malate	copolymer ratio: β-malic acid	abbreviation
poly(benzyl β-malate)	100			$PMLABz_{100}$
poly(benzyl β-malate)-*co*-(butyl β-malate)	90	10	--	$PMLABz_{90}Bu_{10}$
poly(benzyl β-malate)-*co*-(butyl β-malate)	30	70	--	$PMLABz_{30}Bu_{70}$
poly(butyl β-malate)		100	--	$PMLABu_{100}$
poly(β-malic acid)-*co*-(butyl β-malate)		70	30	$PMLAH_{30}Bu_{70}$
poly(β-malic acid)-*co*-(butyl β-malate)		10	90	$PMLAH_{90}Bu_{10}$
poly(β-malic acid)			100	$PMLAH_{100}$
poly(benzyl β-malate)-*co*-(β-malic acid)	20		80	$PMLABz_{20}H_{80}$
poly(benzyl β-malate)-*co*-(β-malic acid)	80		20	$PMLABz_{80}H_{20}$
poly(benzyl β-malate)-*co*-(β-malic acid)	90		10	$PMLABz_{90}H_{10}$

Scheme 2. Synthetic Route for Poly(β-malic acid) from Aspartic Acid[8]

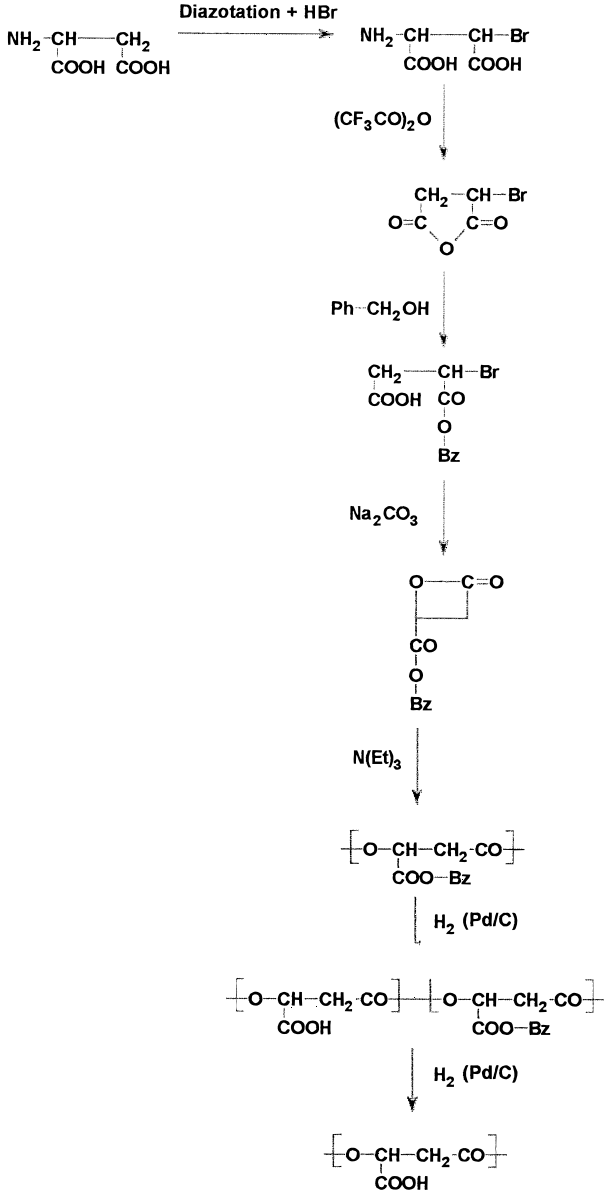

O 1s regions were recorded for all poly(β-hydroxy acids) samples. The analyzer was operated in the fixed analyzer transmission mode with a pass energy of 50 eV (for survey scans) or 20 eV for (C 1s and O 1s envelopes. Data acquisition and analysis were performed by a VGS 5000 data system based on a DEC PDP 11/73 computer.

ToF-SIMS analysis was performed using a VG Ionex IX23S instrument based on the Poschenrieder design, which has been described in detail elsewhere.[16] A 30 keV Ga^+ primary ion beam was used at an incident angle of 38° to surface normal. The secondary ions were accelerated to ±5 keV for the analysis

Table 2. Theoretical and Experimental Atomic Percentages of Poly(β-malic acid) and Its Derivatives

polymer	atomic percentages: theor % C	theor % O	exp % C	exp % O
$PMLABz_{100}$	73.3	26.7	73.2	26.7
$PMLABz_{90}Bu_{10}$	72.8	27.2	72.2	27.8
$PMLABz_{30}Bu_{70}$	69.0	31.0	69.9	30.1
$PMLABu_{100}$	66.7	33.3	66.9	33.1
$PMLAH_{30}Bu_{70}$	63.0	37.0	64.5	35.5
$PMLAH_{90}Bu_{10}$	52.4	47.6	53.3	46.7
$PMLAH_{100}$	50.0	50.0	57.3	42.6
$PMLABz_{20}H_{80}$	57.4	42.6	65.3	34.7
$PMLABz_{80}H_{20}$	70.6	29.4	71.0	29.0
$PMLABz_{90}H_{10}$	72.0	28.0	70.4	29.6

by applying a bias to the sample. For each sample, both positive and negative secondary ion spectra were collected using a total primary ion dose of 1×10^{11} ions cm^{-2}. Such a dose lies well below the damage threshold value of 1×10^{13} ions cm^{-2} for static SIMS.[17] A DEC PDP 11 computer system was used for spectral acquisition, storage, and data processing.

Sample Preparation. Samples were prepared for XPS analysis as films on aluminum foil by casting 2×100 μL drops from 1−2% w/v chloroform solutions (HPLC grade, FSA). Samples were prepared for ToF-SIMS analysis as thin films on aluminum foil from 0.1 % w/v solution in chloroform (HPLC grade, FSA). Prior to analysis, the cast films were irrigated with hexane (HPLC grade, FSA), in order that any poly(dimethylsiloxane) (PDMS) contamination would be removed.

Results and Discussion

XPS Analysis. The XPS analysis of the copolymers of poly(β-malic acid) and its derivatives detected only carbon and oxygen in their survey spectra. The lack of signal arising from the underlying substrate in the wide scans of all the polymers indicated continuity of the polymer films. The theoretical and experimental atomic percentages for the polymer series can be seen in Table 2. It can be seen that the experimental C and O concentrations for the homopolymers $PMLABz_{100}$ and $PMLABu_{100}$ and their copolymers closely matched their theoretical values within the limits of experimental error. However, the experimental carbon composition for the $PMLAH_{100}$ homopolymer and its copolymers was higher than expected, with the exception of $PMLABz_{80}H_{20}$ and $PMLABz_{90}H_{10}$. The higher experimental carbon composition may be attributed to adventitious hydrocarbon deposition or alternatively to the incomplete hydrogenolysis of the benzyl ester in the copolymer synthesis.

The C 1s spectra of the homopolymers $PMLABz_{100}$, $PMLABu_{100}$, and $PMLAH_{100}$ are shown in Figure 1. The C 1s spectra of $PMLABz_{100}$, $PMLABu_{100}$, and their copolymers were fitted with components which were associated with hydrocarbon (C^1−C/C^1−H), the beta-shifted carbon directly bonded to the backbone ester

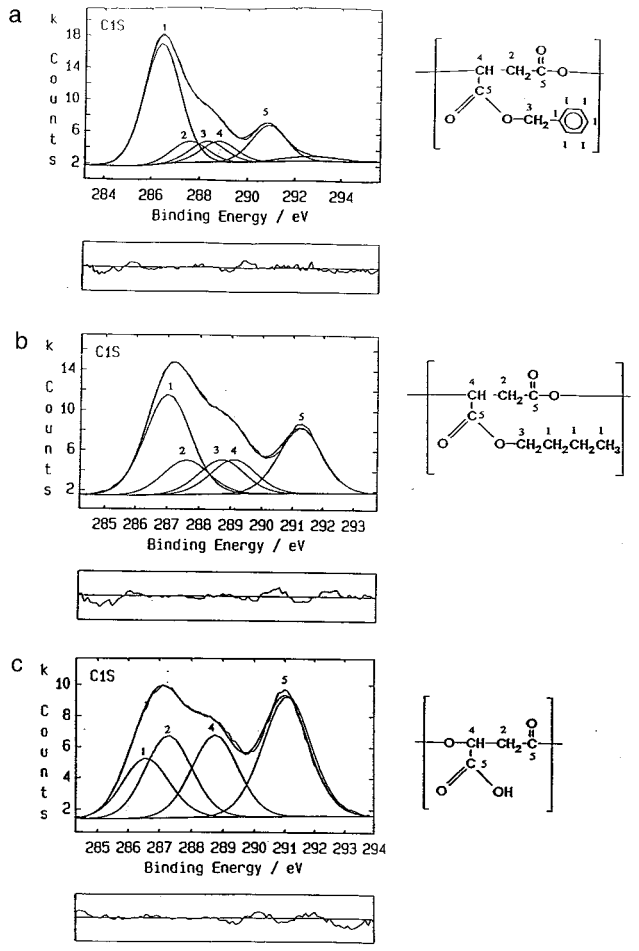

Figure 1. C 1s XPS spectra of the homopolymers (a) $PMLABz_{100}$, (b) $PMLABu_{100}$ and $PMLAH_{100}$.

carbon (C^2-CO_2), the aliphatic carbon associated with the pendant ester (C^3-O), the backbone carbon directly attached to the pendant ester (C^4-CO_2), and the carbon associated within the ester (C^5-O_2).

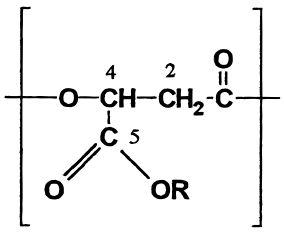

In addition, a further component was included in the C 1s spectra of the polymers containing the PMLABz unit associated with the $\pi-\pi^*$ shake up satellite of the aromatic moiety. The C 1s spectrum of the $PMLAH_{100}$ homopolymer was fitted with the components listed above, with the exception of the aliphatic carbon associated with the pendant esters (C^3-O). Although there is no hydrocarbon (C^1-C/C^1-H) associated within the theoretical structure of the $PMLAH_{100}$ homopolymer, this component was fitted to its C 1s spectrum, as the experimental atomic percentages (listed in Table 2) indicated the possibility of the sample being contaminated with adventitious hydrocarbon. The curve-fitting procedure also involved the fixing of the relative peak areas of the (C^2-CO_2) and (C^4-CO_2) components in a 1:1 ratio, in accord with their theoretical stoichiometric ratio.

Table 3. Relative Binding Energies of the Carbon Components Fitted to the C 1s Spectra of Poly(β-malic acid) and Its Derivatives

	C^1-C/C^1-H	C^2-CO_2	C^3-O	CO^4-CO_2	C^5-O_2
$PMLABz_{100}$	285.0	1.2	1.9	2.4	4.4
$PMLABz_{90}Bu_{10}$	285.0	0.9	2.0	2.4	4.4
$PMLABz_{30}Bu_{70}$	285.0	0.9	1.9	2.2	4.3
$PMLABu_{100}$	285.0	0.6	1.7	2.1	4.3
$PMLAH_{30}Bu_{70}$	285.0	0.8	1.6	2.4	4.4
$PMLAH_{90}Bu_{10}$	285.0	0.8	1.7	2.4	4.6
$PMLAH_{100}$	285.0	0.7		2.1	4.4
$PMLABz_{20}H_{80}$	285.0	0.6	1.6	2.4	4.6
$PMLABz_{80}H_{20}$	285.0	0.9	1.7	2.5	4.5
$PMLABz_{90}H_{10}$	285.0	1.1	1.8	2.6	4.5

The relative binding energies of the components fitted to the C 1s spectra of this polymer series are listed in Table 3. Due to the electrostatic charging of samples, it was necessary for the spectra to be corrected by referencing to the hydrocarbon (C^1-C/C^1-H) peak at 285.0 eV. It has been previously reported that the binding energy of the β-shifted (C^2-CO_2) carbon in polyesters is ~0.7 eV.[18] It can be seen that the (C^2-CO_2) carbon in the $PMLABz_{100}$ homopolymer and the copolymers with greater than 20% PMLABz has a binding energy of nearer 1.0 eV. In the C 1s spectra of the other polymers, the (C^2-CO_2) carbon has a binding energy of within ±0.1 eV of the value reported in the literature.[18] Data from the high-resolution XPS analysis of polymers using the Scienta ESCA300 instrument has reported that there is a significant binding energy shift of ~0.4 eV between aliphatic and aromatic (C^1-C/C^1-H) hydrocarbons.[19] Thus, in the case of the polymers containing a high proportion of the PMLABz monomer, the (C^1-C/C^1-H) hydrocarbon, although corrected to 285.0 eV, may in reality be between 285.0 and 284.6 eV, depending on the proportion of the PMLABz monomer present. This would account for the higher than expected binding energy shift of the β-shifted (C^2-CO_2) carbon in the C 1s spectra of the polymers containing a high percentage of the PMLABz monomer. It can be seen in Table 3 that the higher the proportion of the PMLABz monomer within the polymer, the greater the binding energy of the (C^2-CO_2) carbon, with the homopolymer $PMLABz_{100}$ having the highest shift of 1.2 eV.

The binding energy shift of the aliphatic carbon associated with the pendant esters (C^3-O) in methacrylates has been reported as being ~1.6 eV.[19] When the effect of the presence of aromatic hydrocarbon (C^1-C/C^1-H) within the C 1s spectra is corrected for, it can be seen that the binding energy shift of the aliphatic (C^3-O) carbon in this series of polyesters was found to be 1.6 ± 0.1 eV.

The binding energy shift of the backbone carbon directly bonded to the ester oxygen and pendant methyl group in the polyester poly(hydroxy butyrate) has been reported as being ~1.8 eV.[19] It can be seen from the data in Table 3 that the binding energy shift of the back bone carbon directly attached to the ester oxygen and the pendant ester (C^4-CO_2) is higher than expected, even when the presence of aromatic hydrocarbon (C^1-C/C^1-H) is corrected for. This higher than expected binding energy shift and the wide range of values observed in Table 3 for the (C^4-CO_2) carbon may possibly be the result of a β-shift induced by the pendant group.

The carbon associated within the esters (C^5-O_2) has been reported as being ~4.0 ± 0.2 eV.[19,20] It can be seen from Table 3 that after correcting for the presence of

Table 4. Theoretical and Experimental Values of Carbon Components in the C 1s Spectra of the Poly(β-hydroxy acids)

	theor %					exp %				
	1 C^1-C/C^1-H	2 C^2-CO_2	3 C^3-O	4 CO^4-CO_2	5 C^5-O_2	1 C^1-C/C^1-H	2 C^2-CO_2	3 C^3-O	4 CO^4-CO_2	5 C^5-O_2
$PMLABz_{100}$	54.5	9.1	9.1	9.1	18.2	54	9	9	9	16
$PMLABz_{90}Bu_{10}$	53.3	9.3	9.3	9.3	18.6	53	9	9	9	17
$PMLABz_{30}Bu_{70}$	43.8	11.2	11.3	11.2	22.4	46	11	11	11	20
$PMLABu_{100}$	37.5	12.5	12.5	12.5	25.0	37	13	13	13	24
$PMLAH_{30}Bu_{70}$	30.9	14.7	10.3	14.7	29.4	32	15	11	15	27
$PMLAH_{90}Bu_{10}$	6.8	22.7	2.3	22.7	45.4	9	23	3	23	43
$PMLAH_{100}$		25.0		25.0	50.0	17	23		23	37
$PMLABz_{20}H_{80}$	22.2	18.5	3.7	18.5	37.0	33	19	4	19	25
$PMLABz_{80}H_{20}$	50.0	10.4	8.3	10.4	18.9	48	11	8	11	19
$PMLABz_{90}H_{10}$	52.4	9.7	8.7	9.7	19.5	49	10	9	10	19

aromatic hydrocarbon (C^1-C/C^1-H) is corrected for, the binding energy shift of the (C^5-O_2) carbon was higher than expected at ~4.4 ± 0.2 eV. The presence of thr (C^5-O_2) carbon in both the polyester backbone and the pendant group results in the binding energy shift observed at ~4.4 ± 0.2 eV, being influenced by varying environments depending on the monomers present in the polymer. Thus, the increase in binding energy shift of the (C^5-O_2) carbon is probably due to some influence of the pendant group. This is highlighted by the fact that the highest binding energy shifts observed for the (C^5-O_2) carbon were observed in the C 1s spectra of polymers with a high proportion of PMLAH.

The experimental and theoretical values for the carbon components discussed above are shown in Table 4. It can be seen that, as with the theoretical and experimental C and O atomic percentages for the polymer series, the experimental carbon component concentrations for the homopolymers $PMLABz_{100}$ and $PMLABu_{100}$ and their copolymers closely matched their theoretical values within the limits of experimental error. However, the experimental hydrocarbon (C^1-C/C^1-H) composition for the $PMLAH_{100}$ homopolymer and the copolymer $PMLABz_{20}H_{80}$ was higher than expected and the experimental (C^5-O_2) carbon composition was lower than expected. This is also in agreement with the experimental carbon atomic percentages shown in Table 2 and may be attributed to either adventitious hydrocarbon or the incomplete hydrogenolysis of the benzyl ester. Alternatively, it is possible that with a low proportion of the benzyl ester being present in the copolymer a surface orientation effect is being observed. It is also interesting to note that although the experimental (C^5-O_2) component was lower than expected, all the other carbon components were in agreement with theoretical values, within the limits of experimental error.

The O 1s spectra of these polymers were assumed to consist of two components associated with the ester oxygen and the carboxyl oxygen. It was observed that the O 1s spectra were symmetrical, which was expected due to both components being in a 1:1 ratio, as calculated from the theoretical stoichiometry.

ToF-SIMS Analysis. ToF-SIMS spectra were acquired for all the poly(β-hydroxy acids) under investigation in both the negative and positive ion modes. For clarity the negative and positive ion ToF-SIMS spectra will be discussed separately.

Negative Ion ToF-SIMS Spectra. The negative ion ToF-SIMS spectra of all the homo- and copolymers were somewhat similar in the region *m/z* 0−100. As is the case with most polymers containing oxygen, the most dominant ions in this region were at *m/z* 16 and 17, which can be assigned to O^- and HO^-, respectively.

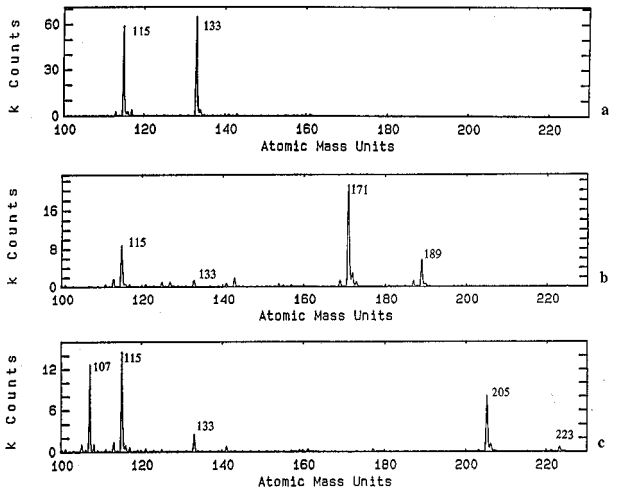

Figure 2. Negative ion ToF-SIMS spectra of the homopolymers (a) $PMLAH_{100}$, (b) $PMLABu_{100}$, and (c) $PMLABz_{100}$; *m/z* 100−230.

Other ions observed in this mass region include those at *m/z* 41/43, 71/73, and 87, which can be assigned to $C_2HO^-/C_2H_3O^-$, $C_3H_3O_2^-/C_3H_5O_2^-$ (with $C_4H_7O^-/C_4H_9O^-$ contributions for the PMLABu-containing polymers), and $C_3H_3O_3^-$, respectively.

The negative ion ToF-SIMS spectra of the homopolymers $PMLAH_{100}$, $PMLABu_{100}$, and $PMLABz_{100}$ in the region *m/z* 100−230 are shown in Figure 2. In this mass region the negative ion ToF-SIMS spectrum of $PMLAH_{100}$ has two diagnostic ions at *m/z* 115 and 133. The ion at *m/z* 115 can be assigned to $[M_{PMLAH}-H]^-$, and the ion at *m/z* 133 can be assigned to $[M_{PMLAH}+OH]^-$, which have the structures below.

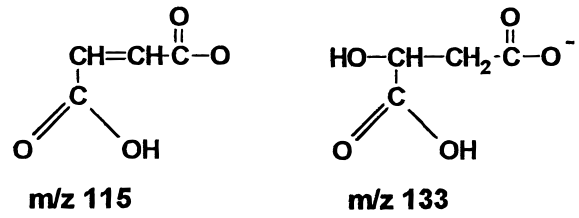

In the *m/z* 100−200 region of the $PMLABu_{100}$ negative ion ToF-SIMS spectrum (as shown in Figure 2b), the ions at *m/z* 115 and 133 formed by side chain cleavage were also observed (i.e. $[M_{PMLABu}-C_4H_9]^-$ and $[M_{PMLABu}-C_4H_9+H_2O]^-$, respectively). Additional ions were observed at *m/z* 171 and 189, which can be assigned to $[M_{PMLABu}-H]^-$ and $[M_{PMLABu}+OH]^-$, which have the structures below.

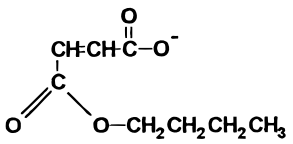

m/z 171

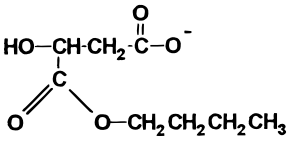

m/z 189

In the same mass region, the negative ion ToF-SIMS spectrum of the homopolymer $PMLABz_{100}$ (as shown in Figure 2c) also shows the presence of ions at m/z 115 and 133 arising from side chain cleavage, as well as additional ions at m/z 107, 205, and 223. The ion at m/z 107 corresponds to $C_6H_5CH_2O^-$, generated by cleavage in the pendant benzyl ester group. The ion at m/z 205 can be assigned to the $[M_{PMLABz} - H]^-$ ion for PMLABz, and the ion at m/z 223 may be assigned to the $[M_{PMLABz} + OH]^-$ ion, which have the structures below.

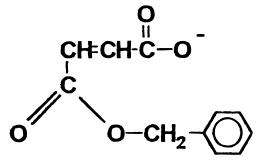

m/z 205

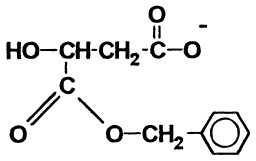

m/z 223

It should be noted that the relative ion intensity of the $[M_{PMLABu} - H]^-$ ion at m/z 171 is much greater than that of the ion at m/z 115. In contrast, the relative intensity of the $[M_{PMLABz} - H]^-$ ion at m/z 205 is lower than that of the ion at m/z 115. This latter observation is attributed primarily to the dominant fragmentation at the benzylic bond in the pendant benzyl ester group of the PMLABz polymer.

Figure 3 shows the negative ion ToF-SIMS spectra in the region m/z 100−230 for the homo- and copolymers of PMLABz and PMLAH. It can be seen that the most dominant ions in the spectra of this copolymer series were those at m/z 115 and 133, respectively. However, as the concentration of the PMLABz component increased, the relative intensities of the $C_7H_7O^-$ and $[M_{PMLABz} - H]^-$ ions at m/z 107 and 205 also increased. This indicates the ions diagnostic of PMLABz increased in relation to the copolymer composition.

Figure 4 shows the negative ion ToF-SIMS spectra in the mass region m/z 100−230 for the copolymers of PMLABu and PMLAH. It can be seen that the most dominant ion in the spectra of the $PMLAH_{1-x}Bu_x$ copolymers is at m/z 115 ($[M_{PMLAH} - H]^-/[M_{PMLABu} - C_4H_9]^-$). As was observed in the spectra acquired from the copolymers of PMLAH and PMLABz, the relative intensity of the ions at m/z 171 and 189, diagnostic of PMLABu, changed in relation to the copolymer composition. It is also interesting to note that the relative intensity of the ion at m/z 133, $[M_{PMLAH} + OH]^-/[M_{PMLABu} - C_4H_9 + H_2O]^-$, which has the same ion structure, changed in relation to the concentration of the PMLABu component. This can also be observed in the spectra acquired from the copolymers of PMLAH and PMLABz (as shown in Figure 3) but was not as markedly noticeable. This indicates that the formation of this ion is dependent on the pendant group and that it is formed least readily when the pendant group is the butyl ester.

Parts b−d of Figure 5 show the negative ion ToF-SIMS spectra in the region m/z 100−230 for the

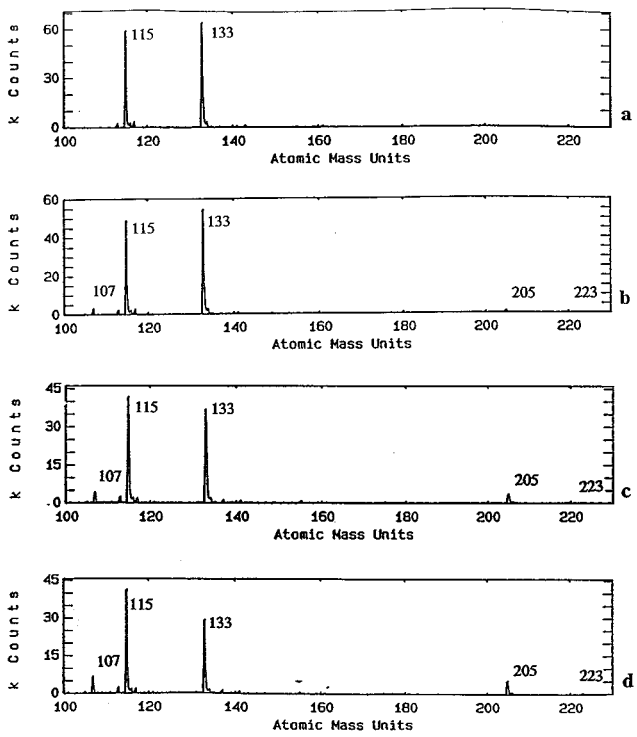

Figure 3. Negative ion ToF-SIMS spectra of (a) the homopolymer $PMLAH_{100}$, (b) the copolymer $PMLABz_{20}H_{80}$, (c) the copolymer $PMLABz_{80}H_{20}$, and (d) the copolymer $PMLABz_{90}H_{10}$; m/z 100−230.

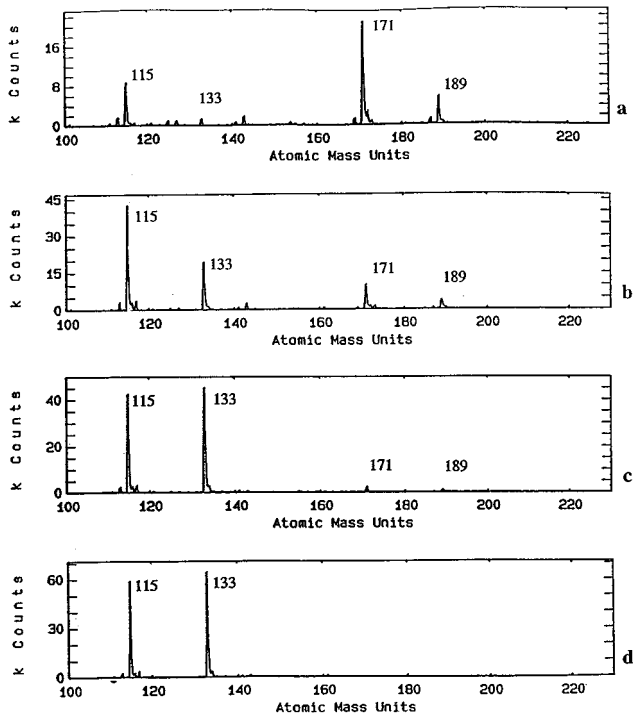

Figure 4. Negative ion ToF-SIMS spectra of (a) the homopolymer $PMLABu_{100}$, (b) the copolymer $PMLAH_{30}Bu_{70}$, (c) the copolymer $PMLAH_{90}Bu_{10}$, and (d) the homopolymer $PMLAH_{100}$; m/z 100−230.

copolymers of PMLABz and PMLABu, where it can be seen that the ions diagnostic of both PMLABu and PMLABz were present. In the spectra of the copolymers with higher proportions of PMLABz, the ions at m/z 205 and 223, diagnostic of PMLABz, were more intense than the ions at m/z 171 and 189, diagnostic of PMLABu. Similarly, in the spectrum of the copolymer

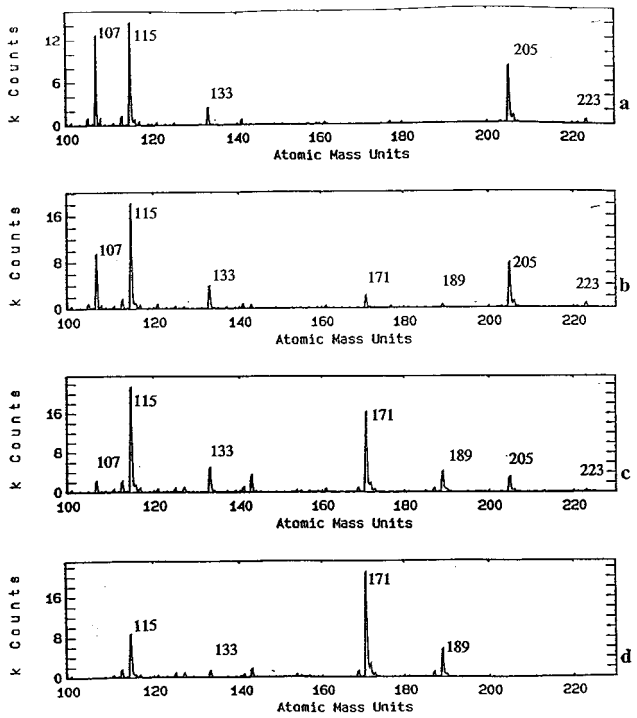

Figure 5. Negative ion ToF-SIMS spectra of (a) the homopolymer $PMLABz_{100}$, (b) the copolymer $PMLABz_{90}Bu_{10}$, (c) the copolymer $PMLABz_{30}Bu_{70}$, and (d) the homopolymer $PMLABu_{100}$; m/z 100−230.

with a higher proportion of PMLABu, the ions at m/z 171 and 189, diagnostic of PMLABu, were more intense than the ions at m/z 205 and 223, diagnostic of PMLABz. This indicates that the relative intensities of diagnostic ions are related to the composition of the copolymers.

Finally, no significant anions were observed above m/z 230 for any of the homopolymers or copolymers. Low-intensity signals observed at m/z 231 and 249 for some of the PMLAH-containing polymers are assigned to $[2M_{PMLAH} - H]^-$ and $[2M_{PMLAH} + OH]^-$, respectively. Extremely weak signals observed at m/z 343 and 361, for some of the PMLABu-containing polymers, may correspond to $[2M_{PMLABu} - H]^-$ and $[2M_{PMLABu} + OH]^-$, respectively.

Positive Ion ToF-SIMS Spectra. The positive ion ToF-SIMS spectra of the homopolymers $PMLAH_{100}$ and $PMLABu_{100}$, as shown in parts a and b of Figure 6, respectively, were dominated by $C_xH_y^+/C_xH_yO_z^+$ cations at m/z 27/29, 41/43, 55/57 (where, for $PMLABu_{100}$, the major contributor to the peak at m/z 57 is $C_4H_9^+$, formed by cleavage of the butyl ester side chain), 71/73, 89, and 99 (particularly intense in the case of $PMLAH_{100}$, corresponding to $[M_{PMLAH} - OH]^+$). The positive ion ToF-SIMS spectra of the homopolymer $PMLABz_{100}$ in the m/z 0−100 mass region (as shown in Figure 6c) was different from that observed for the other homopolymers, with the most dominant cation being observed at m/z 91. This ion can be attributed to the $C_7H_7^+$ tropylium ion formed by cleavage, at the benzylic bond, of the benzyl ester side chain.[21]

The positive ion ToF-SIMS spectra of the homopolymers $PMLAH_{100}$, $PMLABu_{100}$, and $PMLABz_{100}$ in the region m/z 100−230 can be seen in Figure 7. It can be seen in Figure 7a that the most dominant cation in this region of the $PMLAH_{100}$ positive ion ToF-SIMS spectrum was observed at m/z 117, which can be attributed

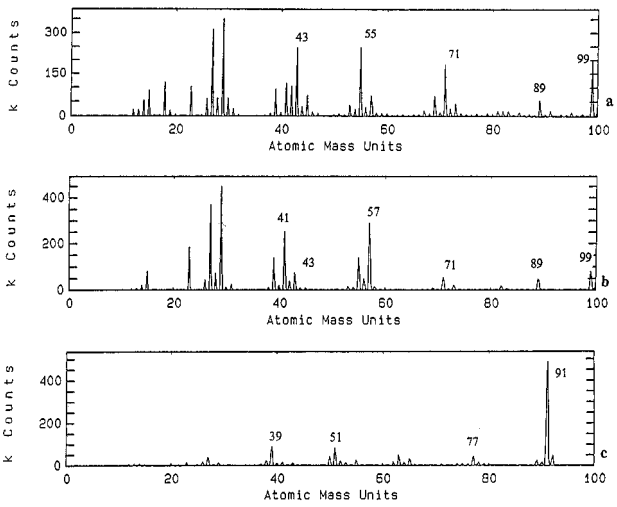

Figure 6. Positive ion ToF-SIMS spectra of the homopolymers (a) $PMLAH_{100}$, (b) $PMLABu_{100}$, and (c) $PMLABz_{100}$; m/z 0−100.

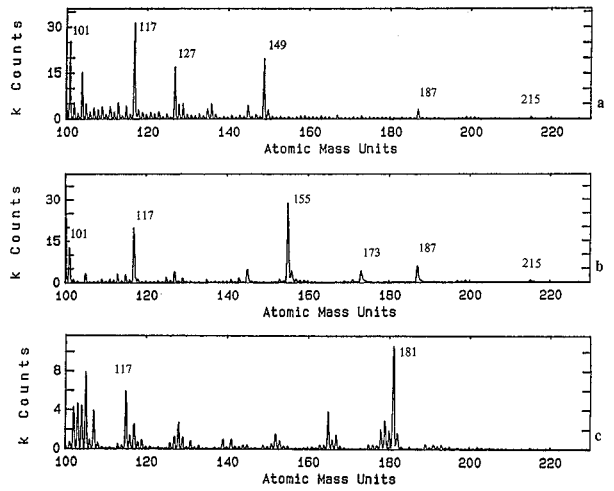

Figure 7. Positive ion ToF-SIMS spectra of the homopolymers (a) $PMLAH_{100}$, (b) $PMLABu_{100}$, and (c) $PMLABz_{100}$; m/z 100−230.

to $[M_{PMLAH} + H]^+$, of the structure below.

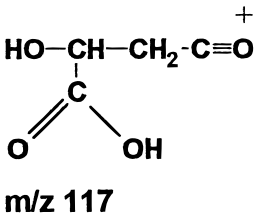

m/z 117

Other ions observed at m/z 187 and 215, for this $PMLAH_{100}$ homopolymer, can be attributed to $[2M_{PMLAH} - CO_2H]^+$ and $[2M_{PMLAH} - OH]^+$, respectively. Additional ions observed at m/z 127 and 149 are attributed to surface contamination, as they were not observed with the same relative intensities within the ToF-SIMS spectra of copolymers with a high PMLAH content.

The dominant cations in the m/z 100−230 region of the $PMLABu_{100}$ positive ion ToF-SIMS spectrum were observed at m/z 117, 155, 173, 187, and 215, as shown in Figure 7b. The cations at m/z 117, 187, and 215 are equivalent to those observed for $PMLAH_{100}$, while the most dominant cations observed at m/z 155 and 173 can be attributed to $[M_{PMLABu} - OH]^+$ and $[M_{PMLABu} +$

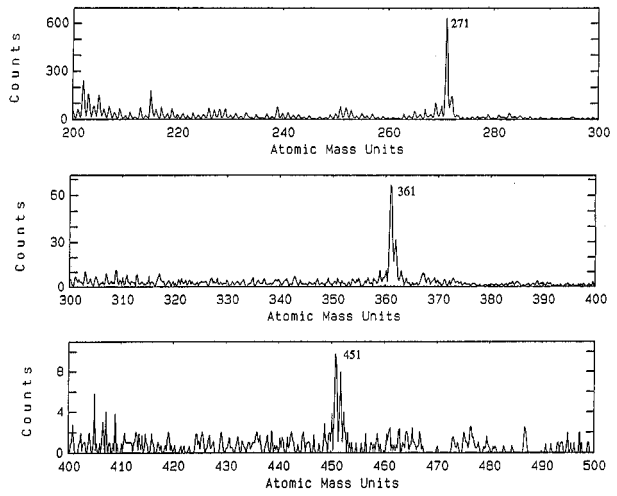

Figure 8. Positive ion ToF-SIMS spectrum of the homopolymer $PMLABz_{100}$; *m/z* 200−500.

$H]^+$, respectively, of the structures below.

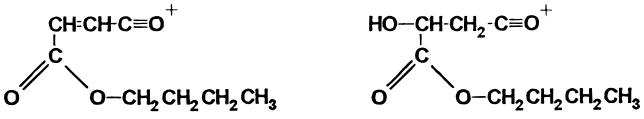

m/z 155 **m/z 173**

The most dominant cation in the *m/z* 100−230 region of the $PMLABz_{100}$ positive ion ToF-SIMS spectra was observed at *m/z* 181, as shown in Figure 7c. It was expected that cations at *m/z* 189 and 207 attributable to $[M_{PMLABz} - OH]^+$ and $[M_{PMLABz} + H]^+$, respectively, would be observed. However, these ions were not detected with any significant intensity in the positive ion ToF-SIMS spectra of any of the polymers containing PMLABz. In addition to the ion at *m/z* 181, other prominent ions were observed at *m/z* 103/105, 115, 128, 152, 165, and 178/179. All of these latter ions are characteristic of aromatic hydrocarbon.[22]

Figure 8 shows the positive ion ToF-SIMS spectrum of $PMLABz_{100}$ in the region *m/z* 200−500. It can be seen that dominant cations were observed at *m/z* 271, 361, and 451. In addition to the cation at *m/z* 181, this indicates successive additions or losses of 90 amu, where the base peak of this series is the tropylium ion at *m/z* 91. These ions were observed to be the most dominant species present in the ToF-SIMS spectra of all the polymers containing PMLABz. Whilst structural assignments for this series of cations have not yet been resolved, the successive differences of 90 amu suggest they might arise from rearrangements involving benzyl ester groups in close proximity.

As the positive ion ToF-SIMS spectra of most of the poly(β-hydroxy acids) containing PMLABz were dominated by the peaks at *m/z* 91, 181, 271, 361, and 451, the remaining discussion will concentrate on the homopolymers $PMLAH_{100}$ and $PMLABu_{100}$ and their copolymers. The *m/z* 100−230 regions of the positive ion ToF-SIMS spectra of the copolymers of PMLAH and PMLABu are shown in Figure 9. It can be seen that these spectra exhibited cations diagnostic of PMLABu at *m/z* 155 and 173, whose relative ion intensities increase as the proportion of PMLABu within the copolymer increases.

Above *m/z* 230, a peak was observed at *m/z* 233, $[2M_{PMLAH} + H]^+$, where an ion of the same structure originates from PMLABu for the homopolymers

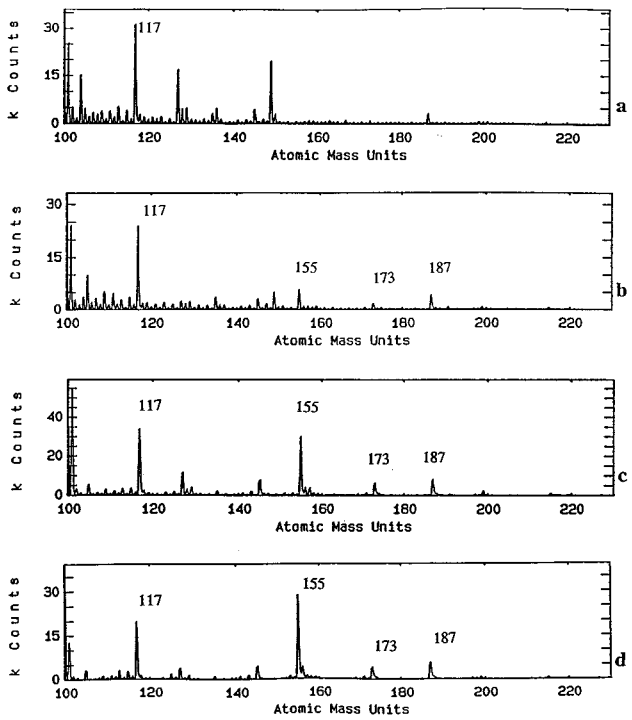

Figure 9. Positive ion ToF-SIMS spectra of (a) the homopolymer $PMLAH_{100}$, (b) the copolymer $PMLAH_{90}Bu_{10}$, (c) the copolymer $PMLAH_{30}Bu_{70}$, and (d) the homopolymer $PMLABu_{100}$; *m/z* 100−230.

$PMLAH_{100}$ and $PMLABu_{100}$ and their copolymers. For all of the PMLABu-containing polymers, peaks were also observed at *m/z* 243, 271, 289, and 327. These are attributed to $[M_{PMLAH} + M_{PMLABu} - CO_2H]^+$ (where an ion of the same structure originates from the $PMLABu_{100}$ homopolymer), $[M_{PMLAH} + M_{PMLABu} - OH]^+$, $[M_{PMLAH} + M_{PMLABu} + H]^+$, and $[2M_{PMLABu} - OH]^+$, respectively.

Conclusions

The use of ToF-SIMS and XPS has given a detailed insight into the surface chemical structure of poly(β-malic acid) and its derivatives. The quantitative elemental data acquired through the XPS analysis of these polymers showed a good correlation between the experimental and theoretical compositions. The peak fitting routine applied to the C 1s spectra provided functional group information. The molecular specificity of ToF-SIMS was shown in the analysis of these materials through the observation of characteristic fragmentation patterns, which consisted of ions diagnostic of the polymers under investigation.

References and Notes

(1) Vert, M. Bioresorbable polymers for temporary therapeutic applications. *Angew. Makromol. Chem.* **1989**, *166/167*, 155.
(2) Vert, M. Biomedical polymers from chiral lactides and functional lactones. *Makromol. Chem., Macromol. Symp.* **1986**, *6*, 109.
(3) Holland, S. J.; Tighe, B. J.; Gould, P. L. Polymers for biodegradable medical devices. 1. The potential of polyesters as controlled macromolecular release systems. *J. Controlled Release* **1986**, *4*, 155.
(4) Vert, M.; Lenz, R. W. Preparation and properties of poly-β-malic acid a functional polyester of potential biomedical importance. *Polym. Prepr.* (*Am. Chem. Soc., Div. Poly. Chem.*) **1979**, *20*, 608.
(5) Ouchi, T.; Fujino, A. Synthesis of Poly(α-malic acid) and its hydrolysis behaviour *in vitro*. *Makromol. Chem.* **1989**, *190*, 1523.

(6) Zhou, Q.; Kohn, J. Preparation of poly(L-serine ester): A structural Analogue of conventional poly(λ-serine). *Macromolecules* **1990**, *23*, 3399.
(7) in't Veld, P. J. A.; Dijkstra, P. J.; Feijen, J. Synthesis of biodegradable polyesteramides with pendant functional groups. *Makromol. Chem.* **1992**, *193*, 2713.
(8) Guerin, P.; Vert, M.; Braud, C.; Lenz, R. W. Optically active poly(β-malic acid). *Polym. Bull.* **1985**, *14*, 187.
(9) Braud, C.; Bunel, C.; Vert, M. Poly(β-malic acid): A new polymeric drug-carrier. Evidence for degradation *in vitro*. *Polym. Bull.* **1985**, *13*, 293.
(10) Walls, J. M. In *Methods of Surface Analysis*; Walls, J. M., Ed.; Cambridge University Press: Cambridge, 1989; p 1.
(11) Duke, C. B. Atoms and electrons at surfaces: a modern scientific revolution. *J. Vac. Sci. Technol. A* **1984**, *2*, 139.
(12) Ratner, B. D. In *The Surface Characterisation of Biomaterials*; Ratner, B. D., Ed.; Elsevier Science Publishers: Amsterdam, 1988; p 13.
(13) Kasemo, B. In *The Surface Characterisation of Biomaterials*; Ratner, B. D., Ed.; Elsevier Science Publishers: Amsterdam, 1988; p 1.
(14) Davies, M. C.; Short, R. D.; Khan, M. A.; Watts, J. F.; Brown, A.; Eccles, A. J.; Humphrey, P.; Vickerman, J. C.; Vert, M. An XPS and SIMS analysis of biodegradable biomedical polyesters. *Surf. Interface Anal.* **1989**, *14*, 115.
(15) Davies, M. C.; Khan, M. A.; Short, R. D.; Akhtar, S.; Pouton, C.; Watts, J. F. XPS and SSIMS analysis of the surface chemical structure of poly(caprolactone) and Poly(β-hydroxybutyrate-β-hydroxyvalerate) copolymers. *Biomaterials* **1990**, *11*, 228.
(16) Eccles, A. J.; Vickerman, J. C. *J. Vac. Sci. Technol.* **1989**, *A7*, 234.
(17) Briggs, D.; Hearn, M. J. Interaction of ion beams with polymer, with particular respect to SIMS. *Vacuum* **1986**, *36*, 1005.
(18) Pijpers, A. P.; Donners, W. A. Quantitative determination of the surface composition of acrylate copolymer latex films by XPS (ESCA). *J. Polym. Sci., Polym. Chem. Ed.* **1985**, *23*, 453.
(19) Beamson, G.; Briggs, D. *High resolution XPS of organic polymers—The Scienta ESCA300 database*; J. Wiley and Sons: Chichester, 1992.
(20) Castner, D. G.; Ratner, B. D. Surface characterisation of butyl methacrylate polymers by XPS and Static SIMS. *Surf. Interface Anal.* **1990**, *15*, 479.
(21) McLafferty, F. W.; Turecek, F. Interpretation of Mass spectra; University Science Books: Mill Valley, CA, 1993.
(22) Briggs, D., Brown, A., Vickerman, J. C., Eds. *Handbook of Static Secondary Ion Mass Spectrometry*; J. Wiley and Sons: Chichester, 1989.

MA9702612